Received: 10 May 2019 | Revised: 8 August 2019 | Accepted: 17 August 2019

DOI: 10.1002/mc.23107

RESEARCH ARTICLE

Molecular Carcinogenesis WILEY

miR-210-3p mediates metabolic adaptation and sustains DNA damage repair of resistant colon cancer cells to treatment with 5-fluorouracil

Erica Pranzini[1] | Angela Leo[1] | Elena Rapizzi[2] | Matteo Ramazzotti[1] | Francesca Magherini[1] | Lisa Giovannelli[3] | Anna Caselli[1] | Paolo Cirri[1] | Maria Letizia Taddei[2] | Paolo Paoli[1]

[1]Department of Experimental and Clinical Biomedical Sciences, University of Florence, Florence, Italy

[2]Department of Experimental and Clinical Medicine, University of Florence, Florence, Italy

[3]Section of Pharmacology and Toxicology, Department of NeuroFarBa, University of Florence, Florence, Italy

Correspondence
Maria Letizia Taddei, Department of Experimental and Clinical Medicine, University of Florence, Viale Morgagni 50, 50134 Firenze, Italy.
Email: marialetizia.taddei@unifi.it

Funding information
Associazione Italiana per la Ricerca sul Cancro, Grant/Award Number: 8797

Abstract

Chemoresistance is the primary cause of chemotherapy failure. Compelling evidence shows that micro RNAs (miRNAs) contribute to reprogram cancer cells toward a resistant phenotype. We investigate the role of miRNAs in the response to acute treatment with 5-FU in colon cancer-resistant cells. We performed a global gene expression profile for the entire miRNA genome and found a change in the expression of four miRNAs following acute treatment with 5-FU. Among them, we focused on miR-210-3p, previously described as a key regulator of DNA damage repair mechanisms and mitochondrial metabolism. We show that miR-210-3p down-regulation enables resistant cells to counteract the toxic effect of the drug increasing the expression of RAD-52 protein, responsible for DNA damage repair. Moreover, miR-210-3p downregulation enhances oxidative phosphorylation (OXPHOS), increasing the expression levels of succinate dehydrogenase subunits D, decreasing intracellular succinate levels and inhibiting HIF-1α expression. Altogether, these adaptations lead to increased cells survival following drug exposure. These evidence suggest that miR-210-3p downregulation following 5-FU sustains DNA damage repair and metabolic adaptation to counteract drug treatment.

KEYWORDS
chemoresistance, DNA damage, miR-210-3p, oxidative phosphorylation, 5-fluorouracil

1 | INTRODUCTION

The aim of all anticancer therapies is to eradicate cancer cells, to prevent organ damage and, as the last event, to promote patient survival. Different types of drugs are available today to achieve this aim. However, despite the abundance of pharmacological weapons, the war against cancer is far to be won.[1] The dissemination and proliferation of cancer-resistant cells are often the main obstacles that prevent the complete eradication of malignant tumors and the first cause of death in cancer patients.[2] For this reason, the development of resistant cells during anticancer therapies is considered a negative prognostic event.

Resistant cells differ from their sensitive counterpart for several aspects: the improved ability to repair DNA damage, the constitutive activation of prosurvival signaling pathways, the overexpression of drug-extrusion pumps, the enhanced ROS scavenger activity, the increased invasiveness and ability to inhibit the cytotoxic activity of immune cells.[2] These findings suggest that deep genetic and epigenetic reprogramming accompanies the transition from a sensitive to a therapy-resistant phenotype.[3] However, which are

Maria Letizia Taddei and Paolo Paoli contributed equally to this work.

the factors that control this phenomenon remain still to be established.

In the last decades micro RNAs (miRNAs), small noncoding RNA molecules which control gene expression, emerged as crucial molecules widely deregulated in human cancer cells.[4] More importantly, several preclinical studies demonstrated that the deregulation of miRNAs contributes to modulate the sensitivity of cancer cells toward chemotherapy, immunotherapy, and radiotherapy.[5] These evidence suggest that miRNAs targeting could be used as an auxiliary therapy to inhibit tumor growth or, alternatively, to improve the efficacy of traditional anticancer therapy, avoiding the onset of resistant cancer cells.[6]

To this aim, a deeper knowledge of miRNAs expression profile is a fundamental prerequisite to counteract the onset of chemoresistance.

The aim of this study is to characterize miRNA expression levels in colon cancer cells resistant to 5-FU during acute treatment with the drug. This approach has been selected to mimic what occurs in patients that undergo relapse and are treated with this chemotherapeutic agent.[7]

We have previously demonstrated that colon cancer-resistant cells acutely treated with 5-FU modulate their metabolism and undergo epithelial-mesenchymal transition, increasing stemness and aggressiveness. Nevertheless, we demonstrated that it is possible to revert resistance of cancer cells by interfering with molecular mechanisms that mediate the adaptive response.[8] Based on this evidence, we speculate that the adaptive response of resistant cells could be modulated by altered miRNA expression. According to this hypothesis, we found that expression levels of four miRNAs significantly changed during acute treatment of resistant cells with 5-FU. Among them, mir-210-3p, which previous studies have indicated as a regulator of cells cycle progression, DNA repair, and metabolism[9] resulted significantly downregulated. Data reported in this manuscript showed that in HT29 human colon carcinoma cells resistant to 5-FU (HT29R) the downregulation of mir-210-3p contributes (a) to enhance the expression of DNA repair proteins such as RAD-52 to counteract drug injury; (b) to rewire the metabolism of resistant cancer cells, by modulating the activity of succinate dehydrogenase (SDH) subunit D and HIF-1-α expression. Together, our results suggest that regulation of mir-210-3p expression is functional to allow resistant cells to survive, overcoming acute stress induced by 5-FU administration.

2 | MATERIALS AND METHODS

2.1 | Cell lines and materials

HT29 colorectal carcinoma cells were purchased from the European Collection of Authenticated Cell Cultures (ECACC). Cells were routinely grown in Dulbecco's Modified Eagle's Medium (DMEM) supplemented with 10% fetal bovine serum, glutamine, and penicillin-streptomycin (Sigma-Aldrich, St. Louis, MO), in a humidified atmosphere with 5% CO_2 at 37°C. HT29 cells resistant to 5-FU (HT29R) were selected by exposing HT29 parental cells to increasing doses of 5-FU during 6 months until the final concentration of 20 μM, as previous described.[8] To ensure the maintenance of resistance to 5-FU, HT29R cells were treated every 15 days with a single dose of the drug (20 μM 5-FU) and let them recover for 1 week before performing experiments.

Unless specified, all reagents were from Sigma-Aldrich. Anti-RAD-52 antibodies were from Abcam (Cambridge, UK), anti-γ-H2AX antibodies were from Cell Signaling (Leiden, The Netherlands); SDHD antibodies were from Merck Millipore (Burlington, MA); anti-Actin and HIF-1α antibodies were from Santa Cruz Biotechnology (Santa Cruz, CA).

2.2 | Western blot analysis

Cells were lysed on ice in radioimmunoprecipitation assay (RIPA) buffer (50 mM TrisHCl pH 7.5, 150 mM NaCl, 100 mM NaF, 2 mM EGTA, 1% triton X-100, 10 μL/mL protease and phosphatase inhibitor; Sigma-Aldrich), 20 to 50 μg of total proteins were loaded on SDS-PAGE gels and transferred to PVDF membranes (BioRad, Hercules, CA). Membranes were incubated overnight at 4°C with the primary antibody. After washing in PBS-Tween 20 (0.1%) membranes were incubated with the appropriate horseradish peroxidase-conjugated secondary antibodies (Santa Cruz Biotechnology) for 1 hour. Proteins were detected using Clarity Western ECL (BioRad) and images were acquired by using Amersham Imager 600 luminometer (Amersham, Buckinghamshire, UK). Quantification of bands was carried out by using the Amersham quantification software.

2.3 | Immunoprecipitation

Cells (4×10^5) were seeded in 60 mm plates and lysed on ice in 300 μL of RIPA buffer. Lysates were centrifuged at 4°C, 14 000 rpm for 15 minutes: supernatants were collected. After protein quantification with bicinchoninic acid protein assay (Sigma-Aldrich), 400 μg of proteins were immunoprecipitated overnight, at 4°C with the specific anti-RAD-52 antibody (1:100). Then Protein A/G PLUS-Agarose (Santa Cruz Biotechnology) was added and incubated at 4°C for 1 hour. Immunocomplexes were collected and analyzed by Western blot analysis.

2.4 | Transfection

miR-210 mimic (Pre-miR, catalogue number 4464066; ID HC10516) was purchased from Life Technologies (Carlsbad, CA), miRCURY LNA Inhibitor (catalogue number 414949-00) was from Exiqon, Quiagen (Hilden,Germany). Cells were transfected as previously described[10] using Lipofectamine RNAiMAX Reagent (Quiagen). miR-210 mRNA expression was assessed by quantitative real-time polymerase chain reaction (qRT-PCR) using miScript SYBR Green PCR Kit.

2.5 | miRNA expression profiling using microarray technique

The global expression data of miRNAs were analyzed using the Agilent Human miRNA Microarray Kit. Such chips (Release 21.0, 8 × 60 K, code G4872A, AMADID 070156) (Agilent, Santa Clara, CA) contains 60-mer probes printed with the Agilent SurePrint technology and can monitor 2549 human miRNAs simultaneously. The RNA was labeled, hybridized and scanned, then probe intensities were obtained using Agilent Feature Extraction software and further analyzed in terms of quality control and normalization with Agilent GeneSpring GX software at the Microarray Facility of the Laboratory for Advanced Therapy Technologies. For statistical analysis, a between-array normalization was performed using 90 the percentile intensity of noncontrol probes. Differential analysis at the probe level was performed by one-way Analysis of Variance (ANOVA) (three groups: HT29, HT29R, HT29R+ 5-FU) with Newman-Keuls post-hoc correction. *P* values from ANOVA were adjusted for multiple testing using the Benjamini-Hochberg procedure. Two group comparisons (HT29/HT29R and HT29R/HT29R+5-FU) were performed with Welch *t* tests. *P* values from *t* tests were adjusted for multiple testing using the Benjamini-Hochberg procedure. Only genes with an adjusted $P < .05$ and a fold change of at least 1.5 (up or down) were considered for further analyses. For the subsequent functional analysis, the target genes of the differentially expressed individual miRNAs (DE) were extracted from miRTarBase database, which only includes genes with an experimental validation (PMID 29126174). Functional analysis was performed on the sets of DE miRNA resulting from two-group comparisons. For each comparison, three different sets of miRNAs were considered: the entire pool of DE miRNA, the upregulated DE miRNAs, and the downregulated DE miRNAs. For each set, the target genes shared by at least two of the miRNAs were included in the functional analysis, so that the population size of genes under testing was of adequate size. Functional analysis was performed against gene sets available at the Broad Institute MsigDb database (PMID 16199517) using the Fisher Exact Test using all genes of the gene sets as the sample universe. The correction for multiple tests was performed according to the Benjamini-Hochberg procedure. Only gene sets with an adjusted *P* value lower than 0.05 were considered as significantly enriched.

2.6 | Real-time PCR

Total RNA, including small RNAs, was enriched and purified from cells using the miRNeasy Kit (Qiagen, Hilden, Germany) according to the manufacturer's instructions. Total RNA amount was quantified at NanoDrop Microvolume Spectrophotometers and Fluorometer. The reverse transcription reaction of 1 μg of total RNA was carried on using miScript II RT Kit and the quantification of miR-210-3p expression level was assessed by Real-Time PCR using miScript SYBR Green PCR Kit and miScript Primer Assay-HsmiR-210-3p. SNORD61 was used as normalizer (miScript Primer Assay-HsSNORD61; Qiagen). All the amplifications were run on 7500 Fast Real-Time PCR System. Data were reported as relative quantity with respect to the calibrator sample using the $2^{-\Delta\Delta C_t}$ method.

2.7 | Cell cycle analysis

The cell cycle analysis was carried out using cytofluorimetric method. Briefly, HT29R cells were grown in the presence or absence of 20 μM of 5-FU for the specified times, then cells were fixed in 70% cold ethanol. After cells were resuspended in a buffer containing 0.05 mg/mL propidium iodide, 5 μg/mL RNAase A, 0.2% v/v Nonidet P-40, 0.1% sodium citrate. Samples were analyzed by FACScan Flow Cytometer Apparatus (BD Biosciences, San Jose, CA) and ModFit Software (BD Biosciences) was used to determine the cell cycle distribution.

2.8 | Growth rate and doubling time calculation

For cell proliferation analysis, the HT29 and HT29R cells were seeded in six-well plates and cultured in the presence of 10% FBS for 72 hours. Twenty-fourhours after seeding, 20 μM of 5-FU was added to the growth medium. Cells were harvested by trypsinization at various times and counted. The cell numbers were averaged over three independent experiments. Doubling time (Td) was extrapolated using the following formula:

$$Td = 24 \times \frac{lg2}{\lg(n\ \ cellT1) - lg(n\ \ cellT2)}$$

2.9 | Cloning assay

After 24 hours treatment, 1000 cells were seeded into six-well plates and cultured for 9 to 11 days. Subsequently, cells were fixed and stained with a solution containing 1% crystal violet (Sigma-Aldrich) and 10% methanol. Colonies were photographed and counted using ImageJ imaging system. The number of colonies arose after incubation was calculated as a surviving fraction (SF):

$$SF = \frac{n\ \ of\ \ colonies\ \ formed\ \ after\ \ incubation}{n\ \ of\ \ cells\ \ seeded \times PE}$$

where PE is the plating efficiency calculated in untreated cells as the ratio of the number of colonies to the number of cells seeded.[11]

2.10 | Annexin V and propidium iodide assay

Apoptosis was determined using Annexin-V-FLUOS Staining Kit from Roche according to manufacturer's instructions. Briefly, cells were collected, washed, and incubated with 100 μL of Annexin-V-FLUOS labeling solution, for 10 to 15 minutes at room temperature. Cells were analyzed by FACSscan Flow Cytometer Apparatus (BD Biosciences). Q1: (PI labeling) necrotic cells; Q2: (PI/Ann.V labeling) late apoptotic cells; Q3: (no labeling) living cells; Q4: (Ann.V labeling) early apoptotic cells.

2.11 | Cell viability assay

A total of 2×10^4 cells were seeded in 24-well plate and treated 24 hours after the seeding. After the treatment for 24, 48, or 72 hours, cells were washed with phosphate-buffered saline (PBS) and 5 mmol/L MTT (3-(4,5-Dimethylthiazol-2-yl)-2,5-diphenyltetrazolium bromide) was added and incubated for 1 hour at 37°C. Alternatively, cells were stained with crystal violet/methanol solution for 20 minutes. Cells were resuspended in 200 μL of dimethyl sulfoxide: wavelength measuring was performed at 595 nm using a spectrophotometer (Microplate Reader 550; BioRad).

2.12 | Comet assay

HT29 parental and resistant cells were treated with 5-FU for 24 hours. After treatment, cells were analyzed for DNA damage by Comet assay as previously described.[12] Briefly, 5×10^4 cell were resuspended in melted LMP agarose (LMA, 1% in PBS) kept at 37°C, transferred onto clear microscopy slides precoated with agarose and covered with 24 × 50 mm coverslips. Cells were lysed at 4°C for 1 hour (lysis solution: NaCl 2.5 M, Na_2EDTA 100 mM, Tris-HCl 10 mM, TritonX-100 1%, pH 10). The obtained nucleoids were then subjected to an alkaline unwinding step by incubating the slides for 20 minutes at 4°C in alkaline electrophoresis buffer (NaOH 300 mM, Na2EDTA 1 mM, pH 13). Following electrophoresis, slides were neutralized with two washes in 0.4 M Tris-HCl, pH 7.4, briefly washed in distilled water and stained with DAPI (1 μg/mL) overnight in the fridge. On the following day, images of the nucleoids were acquired and analyzed by means of a specific image analysis system (Comet Assay IV; Perceptive Instruments, UK). Tail migration values were recorded for 100 randomly chosen cells for each experimental point and averaged. Each experiment was repeated three times and the corresponding values were further averaged for each experimental point and expressed as mean ± SEM.

2.13 | Oxygen consumption rate measurement and extracellular flux analysis

HT29R cells were transfected with miR-210-3p mimic (hsa-miR-210-3p) or LNA-miR-210-3p inhibitor. After 24 hours of transfection, cells were trypsinized, washed with PBS and resuspended in complete DMEM medium at the concentration of 10^6 cells/mL. One milliliter of cell suspension was transferred to an airtight chamber maintained at 37°C and oxygen consumption was measured using a Clark-type O_2 electrode (Hansatech, Narborough,UK). Oxygen content was monitored for at least 10 minutes. The rate of decrease in oxygen content, related to cell number was taken as index of the respiratory capability.

The oxygen consumption rate (OCR, pmolesO_2 consumed/min) and the extracellular acidification rate (ECAR, mpH/min) were determined by using the XF96 Extracellular Flux Analyzer (Seahorse Bioscience, North Billerica, MA) according to manufacturer's instructions. After 24 hours of transfection, 2×10^4 cells/well were plated on XF96-well microplates in standard medium. After one-day incubation, cells were washed three times with an unbuffered assay medium (pH 7.4) and conditioned for 1 hour at 37°C without CO_2. After incubation, extracellular flux (XF) measurements were performed. A Seahorse XF Cell Mito Stress Test was used to evaluate the mitochondrial function in different experimental conditions. Using this kit, parameters of mitochondrial function were determined by directly measuring the OCR of cells after the injection of specific drugs that target components of the electron transport chain (ETC) in the mitochondria. The compounds (oligomycin, FCCP, and a mix of rotenone and antimycin A) were injected in sequence and basal respiration (without drugs), ATP–linked respiration, maximal respiration, and nonmitochondrial respiration were respectively measured. Maximal respiratory capacity was then calculated by subtracting the basal respiration values from maximal respiration values.

2.14 | SDH activity analysis

Cell homogenates (50 μg) were incubated in a phosphate buffer containing sodium azide, 2,6 dichlorophenolindophenol (DCPIP), sodium succinate, and phenazine methosulfate. Complex II specific activity was evaluated by measuring the decrease in absorbance due to the oxidation of DCPIP at 600 nm.[13]

2.15 | Succinate assay

Succinate levels were determined using a Succinate Assay Kit (BioVision, Milpitas, CA) according to the manufacturer's instructions. All data were normalized on cell protein content.

2.16 | Immunocytochemistry

After washing with PBS, cells were fixed with 3.7% formaldehyde solution in PBS for 20 minutes at 4°C. Then, after extensive washes in PBS, cells were permeabilized with 0.1% Triton X-100 in PBS and then stained with anti-human phospho-histone H2AX (S139) antibodies for 1 hour at room temperature and then with Anti mouse Alexa Fluor 488 antibodies. After several washes with PBS, the coverslips were mounted with glycerol plastine and then observed under a confocal fluorescence microscope (Leica, Wetzlar, Germania).

2.17 | Statistical analysis

Statistical analysis of the data was performed by unpaired Student *t* test for pairwise comparison of groups, and by the ANOVA for comparison between more than two groups. One-way ANOVA when only one categorical variable or single factor was considered, two-way ANOVA when two independent variables were involved. All data were expressed as the mean ± SEM. A $P < .05$ was considered statistically significant. Statistical analysis was carried out on biological replicates, as indicated in the figure legends.

3 | RESULTS

3.1 | 5-FU treatment induces miRNAs deregulation in resistant colon cancer cells

To investigate the contribution of miRNAs expression in the acquisition of chemoresistance, we used as a model a HT29 human colon cancer cell line resistant to 5-FU (HT29R). HT29R cells were obtained exposing HT29 cells to increasing doses of 5-FU, as previously described.[8] A profiled miRNA expression analysis on microarray platform pointed out 98 of the 382 considered miRNAs differently expressed between HT29 and HT29R cells (Table S1), thereby confirming that resistant cells undergo strong genetic reprogramming. However, considering that our priority interest is to study the response of resistant cells to drug treatment, we analyzed also the miRNA profile of HT29R cells acutely treated with 5-FU for 72 hours. Microarray analysis highlighted that the acute treatment with 5-FU induces changes in the expression levels of four miRNAs: among these, three are upregulated, and only one downregulated (Table 1). Taken together, these evidence suggested that resistant cells maintain a certain degree of plasticity and modulate the expression of miRNAs in response to drug treatment.

3.2 | miRNA 210 is downregulated in HT29R cells treated with 5-FU

Among the differentially expressed miRNAs between HT29R treated or not with 5-FU, we focused on miR-210-3p, the only miRNA that resulted upregulated after the treatment. miR-210-3p has been previously associated with regulation of energetic metabolism, cell cycle progression, and DNA repair activity.[14] Microarray analysis showed a significant downregulation of miR-210-3p in HT29R cells following the treatment (Table 1). This result was confirmed by qRT-PCR (Figure 1A). To understand whether the downregulation of miR-210-3p is a specific adaptation of resistant cells to the acute treatment with 5-FU, we analyzed miR-210-3p expression in sensitive HT29 cells treated or not with 5-FU. Interestingly, we found that 5-FU exposure does not induce miR-210-3p down-regulation in HT29 cells (Figure 1B), suggesting that its modulation could be a specific response to 5-FU administration in selected resistant cells.

3.3 | miRNA 210-3p regulates cell cycle and improves DNA damage repair of chemoresistant cells

To analyze the effect of 5-FU administration on HT29R, we evaluated its impact on cell cycle progression. According to previously published data,[15] we found that 24 and 48 hours of treatment with 5-FU induce a stronger G1/S phase arrest in sensitive HT29 cells than in resistant ones (Figure 2A). Moreover, 5-FU-induced cell cycle arrest resulted in large differences in apoptosis induction in the two cell lines during treatment, with the highest levels of apoptosis (represented as "Q4" fraction) observed in the parental cells and the lowest in resistant ones (Figure 2B). The effects of 5-FU treatment on cell proliferation were also confirmed by evaluating cell growth rate and doubling time under drug exposure. Coherently, we found that 5-FU treatment significantly decreases the growth rate of sensible cells without affecting resistant cells proliferation (Figure S1A,B). Moreover, colony formation assay revealed a strong decrease in clonogenicity in HT29 cells after the treatment with the drug but not in HT29R cells (Figure S1B), suggesting that 5-FU treatment does not affect self-renewal ability of resistant cells. Accordingly, we found a much higher increase of H2AX phosphorylation (γ-H2AX), a typical marker of DNA damage,[16] in HT29 cells with respect to HT29R cells following 5-FU treatment (Figure 2B-2D). Finally, the comet assay to detect DNA damage shows a pronounced increased tail migration in HT29 cells and not in resistant cells (Figure 2E and 2F). Collectively, these data suggest that resistant cells are prompt to face the drug administration, probably thanks to their increased ability to repair DNA damage. In contrast, parental cells are not able to activate the DNA damage repair machinery necessary to overcome 5-FU treatment, thus accumulating DNA damage and resulting in cell death.

To gain insight into the role of miR-210-3p in DNA damage repair process, HT29R cells were transiently transfected with LNA-miR-210-3p inhibitor to mimic one of the effects of 5-FU treatment (Figure S2A). In accordance with previous data, we observed that HT29R transfected cells show lower phosphorylation of H2AX and increase their ability to repair the damage induced by 5-FU treatment (Figure 3A). Conversely, the overexpression of miR-210-3p (Figure S2B) induces an increase in γ-H2AX levels and prevents the DNA damage recover, as evidenced by H2AX phosphorylation after 16 hours of treatment (Figure 3B).

Interestingly, one of the targets of miR-210-3p is RAD-52,[17] involved in DNA homology-dependent repair.[18] Coherently, RAD-52 expression is induced by 5-FU treatment in HT29R cells (Figure 3C). To gain insight into the role of miR-210-3p on DNA repair mechanism, we transfected HT29R cells with LNA-miR-210-3p inhibitor to mimic the miR-210-3p down-modulation induced by 5-FU treatment. Interestingly, LNA-miR-210-3p inhibitor causes a strong increase in RAD-52 expression similar to 5-FU treatment (Figure 3D). Conversely, the overexpression of miR-210-3p induces a

TABLE 1 Identification of altered miRNA expression by 5-FU exposure in HT29-resistant cells (HT29R)

Systematic name	*P* (Corr)	Fold change direction	FC (abs)
hsa-miR-210-3p	.007982709	Down	1.8944974
hsa-miR-4252	.007982709	Up	89.433014
hsa-miR-642b-3p	.011085268	Up	10.647714
hsa-miR-6792-5p	.007982709	Up	62.204525

Note: miRNAs significantly altered in HT29R cells following the treatment with 5-FU 20 μM for 72 hours. miRNAs were analyzed by global gene expression profile associated with miRNA array (Affimetrix). Significance fold change cutoff: 0.05.

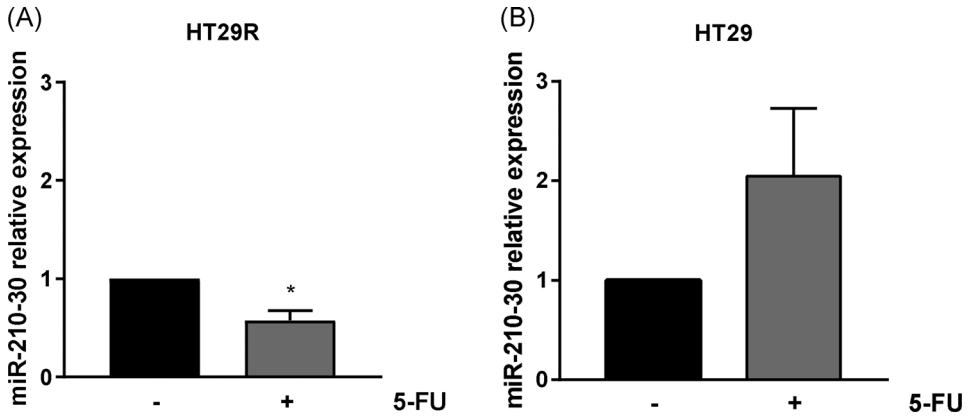

FIGURE 1 miR-210-3p downregulation is an adaptation to 5-FU treatment specific of HT29-resistant cells. qRT-PCR validation of altered expression of miR-210-3p under 5-FU treatment for 72 hours in HT29R resistant cells (A) and HT29 parental cells (B) (data were shown in mean ± SEM; unpaired *t* tests, $^*P < .05$). Untreated conditions are referred to as "–" and 20 μM 5-FU treatments as "+". qRT-PCR, quantitative real-time polymerase chain reaction

decrease in RAD-52 expression (Figure 3E), confirming the critical role of this miRNA in regulating RAD-52 levels.

Taken together, our data suggest that 5-FU- induced miR-210-3p downregulation contributes to DNA damage repair in resistant cells by increasing the expression of the recombination protein RAD-52. To better define the relevance of miR-210-3p downregulation in the response of resistant cells to the insult caused by 5-FU exposure, we evaluated both cell cycle distribution and cell viability after the drug exposure in miR-210-3p overexpressing HT29R cells. We found a cell proliferation arrest in the G1/S phase in HT29R cells overexpressing miR-210-3p after 24 and 48 hours of treatment with 5-FU (Figure 3F). Interestingly, the overexpression of mir-210-3p induces the same cell cycle distribution previously observed in sensible cells after the treatment (Figure 2A). Moreover, MTT viability assay showed that the treatment of HT29R cells overexpressing miR-210-3p with 5-FU causes a slight but significant decrease in cell survival supporting, once again, the requirement of miR-210-3p downregulation to counteract the toxic effect of the drug (Figure 3G).

3.4 | miR-210-3p downregulation enhances SDH activity and sustains metabolic adaptation in resistant cells treated with 5-FU

Previous data from our laboratory showed that metabolic shift towards oxidative phosphorylation (OXPHOS) is one of the major features of HT29R cells responding to 5-FU treatment.[8] Coherently, miR-210-3p modulation also impacts on different steps of mitochondrial metabolism, affecting activity of the ETC complexes.[19,20] Subunit D of mitochondrial succinate dehydrogenase complex (SDHD) is a known target of miR-210-3p.[20] Based on these evidence, we evaluated the effect of 5-FU on SDHD expression. We found that exposure to 5-FU increased SDHD levels in HT29R cells (Figure 4A). Therefore, also total SDH activity is increased by the treatment (Figure 4B). Again, similar effects were observed in HT29R cells transfected with LNA-miR-210-3p inhibitor (Figure 4C and 4D). Moreover, in keeping with the increased activation of SDH, we also observed a lower level of intracellular succinate in HT29R cells treated with 5-FU (Figure 4E).

High levels of succinate have been reported to inhibit prolyl hydroxylase enzymes, thus concurring in HIF-1α stabilization.[21] Furthermore, a strong reciprocal regulation between miR-210-3p and HIF- 1α is well described.[14,22,23] To gain insight to this mechanism, we evaluated HIF-1α levels in HT29 and HT29R cells after 24 hours of treatment with 5-FU. In accordance with the described miR-210-3p downregulation, we found that 5-FU treatment induces a decrease in HIF-1α levels in resistant cells. Conversely, HIF-1α level is not affected by 5-FU treatment in HT29 cells (Figure 5A). To better define the role of HIF-1α in mediating 5-FU resistance, we treated HT29 cells with Topotecan, a widely used HIF-1α inhibitor[24-26] and we evaluated while the inhibition of HIF-1α is sufficient to reproduce the resistant phenotype in sensible cells. Interestingly, we found a strong decrease in 5-FU sensitivity in HT29 cells in the presence of 250 nM of Topotecan (Figure 5B), confirming a detrimental role of HIF-1α in mediating drug resistance.

Altogether these data suggest that miR-210-3p plays a crucial role in the metabolic shift towards OXPHOS of HT29R cells upon treatment with 5-FU. To further corroborate this hypothesis, we used Seahorse technology. The metabolic profile of HT29R cells transfected with LNA-miR-210-3p inhibitor to mimic drug-mediated miR-210-3p downregulation strongly increases the OCR (oxygen consumption rate) (Figure 6A and 6B) without affecting ECAR (Fig. S3A). Specifically, miR-210-3p inhibition induces a strong increase in mitochondrial OCR, calculated by subtracting OCR values following rotenone/antimycin A injection (nonmitochondrial OCR) from basal OCR values (Figure 6C). Oxygen consumption rate was also monitored using a Clark-type O_2 electrode during 10 minutes of incubation. The rate of decrease in oxygen content was found to be higher in LNA-miR-210-3p transfected cells compared to controls (Figure 6G). These results confirm the hypothesis that miR-210-3p downregulation specifically impacts on mitochondrial metabolism of HT29R cells.

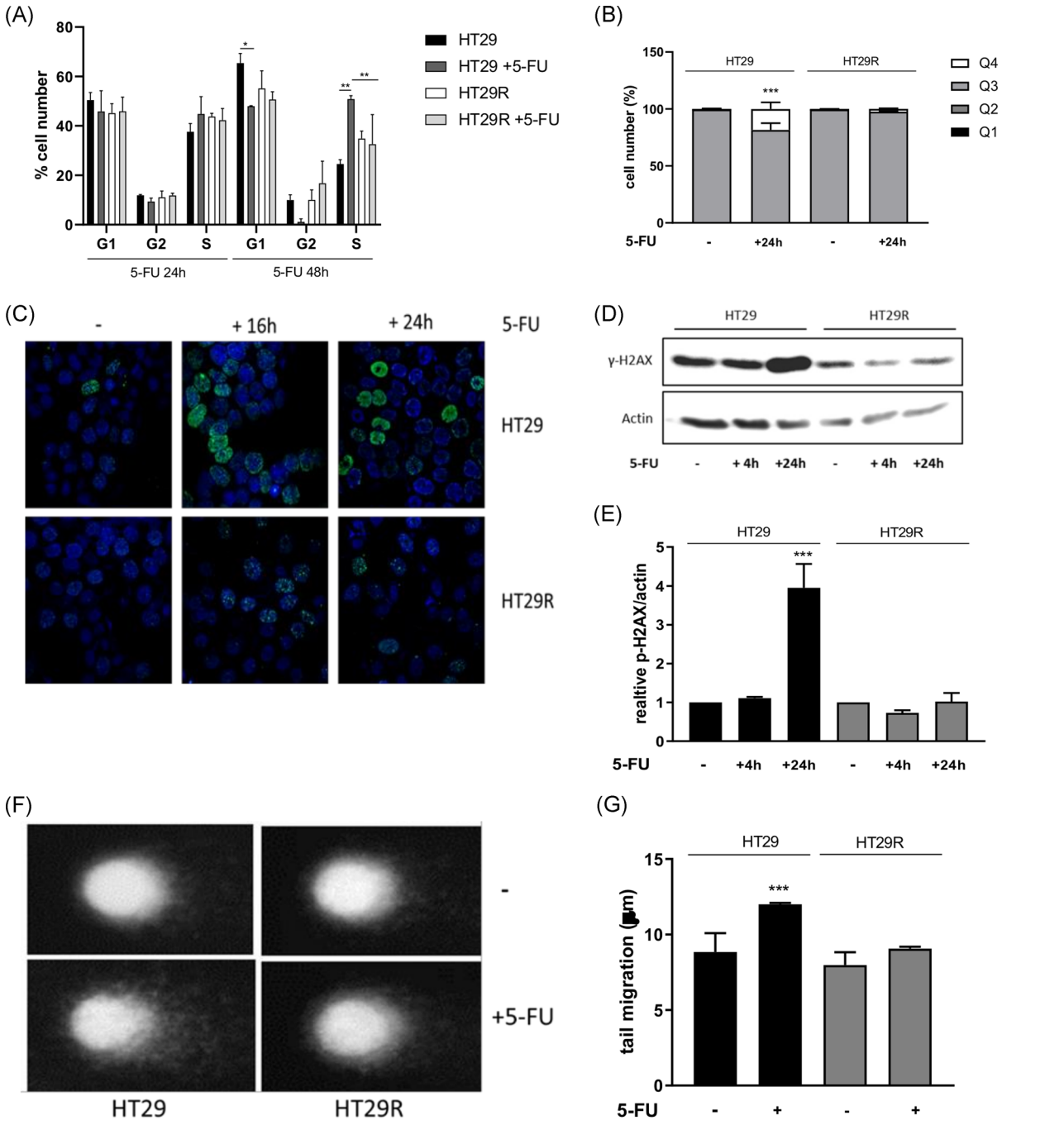

FIGURE 2 DNA damage response in 5-FU-treated parental and resistant HT29 cell lines. (A) Quantitative analysis of cell number percentage of G1, S, and G2/M phase of control cells and cells treated with 20 μM of 5-FU for 24 and 48 hours. HT29 and HT29R cells were stained with PI to analyze the cell cycle distribution by flow cytometry. Quantitation was determined by the area under the indicated phase (data were shown in mean ± SEM; two-way ANOVA, $^{*}P < .05$, $^{**}P < .01$, $^{***}P < .00$). (B) Evaluation of apoptosis in HT29 and HT29R cells. Cancer cells were incubated in the presence of 20 μM 5-FU. After 24 hours, the fraction of apoptotic cells was evaluated using Annexin V/PI assay. For each assay, 10 000 events were acquired. Q1: necrotic cells; Q2: late apoptotic cells; Q3: living cells; Q4: early apoptotic cells. (data were shown in mean ± SEM; one-way ANOVA, $^{***}P < .001$). (C) Representative images of control cells treated or not with 20 μM 5-FU for 16 to 24 hours. Cells were fixed and examined by immunofluorescence for H2AX phosphorylated on Ser139 (γ-H2AX). Nuclei were counterstained with the DNA stain TO-PRO-3. (D) Representative western immunoblotting showing γ-H2AX levels of HT29 and HT29R cells after 24 hours of treatment with 20 μM 5-FU. An anti-actin antibody was used to ensure equal protein loading. (E) The ratio between γ-H2AX and actin expression levels in HT29 and HT29R cells treated with 20 μM 5-FU for the indicated times (data are shown in mean ± SEM; one-way ANOVA, $^{***}P < .001$). (F) Tail migration measured with Comet Assay. HT29 parental and resistant cells were treated with 20 μM 5-FU. After 24 hours cells were resuspended in LMP Agarose, lysed, and nuclear DNA was subjected to electrophoresis. DNA was stained with DAPI (1 μg/mL) (data shown in mean ± SEM; one-way ANOVA, $^{***}P < .001$). (G) Representative images of one Comet Assay experiment. PI, propidium iodide [Color figure can be viewed at wileyonlinelibrary.com]

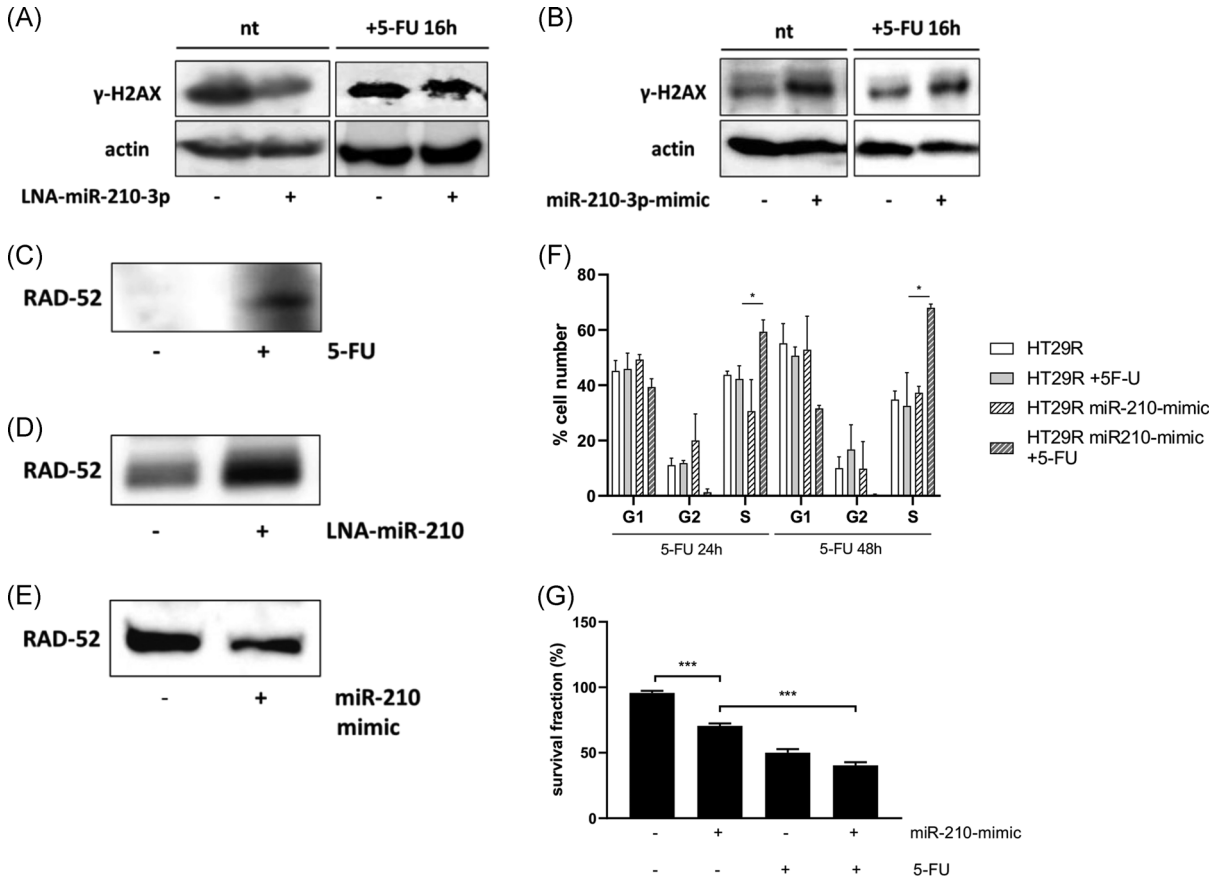

FIGURE 3 miR-210-3p regulates RAD-52 protein levels in resistant cells. Representative western immunoblotting showing levels of γ-H2AX of HT29R cells transfected with LNA-miR-210-3p (A) or with miR-210-3p mimic (B) and treated with 5-FU for 16 hours. An anti-actin antibody was used to ensure equal protein loading. Representative immunoprecipitation analysis of RAD-52 levels after treatment with 5-FU 20 μM for 24 hours (C) and after LNA-miR-210 inhibitor (D) or miR-210-mimic (E) transfection. RAD-52 was immunoprecipitated and analyzed by SDS-PAGE separation and Western blot. An equivalent amount of total protein was loaded on gels. (F) Quantitative analysis of cell number percentage of G1, S, and G2/M phase of HT29R control cells and cells transfected with miR-210-mimic treated with 20 μM of 5-FU for 24 and 48 hours. HT29R cells were stained with PI to analyze the cell cycle distribution by flow cytometry. Quantitation was determined by the area under the indicated phase (data were shown in mean ± SEM; two-way ANOVA, $^{*}P < .05$). (G) Cell viability assay on HT29R cells previously transfected with miR-210-mimic and treated with 20 μM 5-FU 24 hours after transfection. Cells viability was measured by MTT test after 48 hours of treatment (data were shown in mean ± SEM; unpaired *t* test, $^{*}P < .05$, $^{***}P < .001$). ANOVA, Analysis of Variance; PI, propidium iodide

Conversely, the overexpression of miR-210-3p mimic induces a decrease in OCR in resistant cells, evaluated both with Seahorse technology and Clark-type O_2 electrode (Figure 6D and 6H). Coherently with previous data, we found a decrease in OCR/ECAR rate and mitochondrial OCR (Figure 6E and 6F) without any change in ECAR (Figure S3B), suggesting an impairment of mitochondrial activity in transfected cells. Together, these data support that 5-FU increases HT29R mitochondrial metabolism, through the down-modulation of miR-210-3p.

Hence, we tried to interfere with this metabolic adaptation by blocking SHD activity to clarify its relevance in the response of HT29R cells to 5-FU injury. We observed that Harzianopyridone, an SDH inhibitor,[27] reduced survival of resistant cells treated with 5-FU in a dose-dependent manner, while shows the negligible effect on cell survival when used alone (Figure 6I). Altogether, these evidence suggest that miR-210-3p, through SDH induction, could have a role in promoting the survival of resistant cells following treatment with 5-FU.

4 | DISCUSSION

Cancer drug resistance is a major issue facing the current fight against cancer. Over the years, several new approaches have been proposed to overcome the establishment of cancer drug resistance, including the use of drug cocktails instead of mono-drug based therapy. Combined therapies, containing two or three drugs with different mechanisms, are generally more effective than single drug and show stronger antiproliferative effects.[28] However, despite their apparent enhanced efficiency, a large number of patients still develop resistance toward cocktails too and undergo relapse. The appearance of resistant cells is considered a poor prognosis factor, mainly because strongly reduces the therapeutically options useful to achieve the complete eradication of cancer cells.

Several processes have been described to lead to chemotherapeutics resistance, including intrinsic and acquired ones.[1] The intrinsic resistance to anticancer treatments is a characteristic of

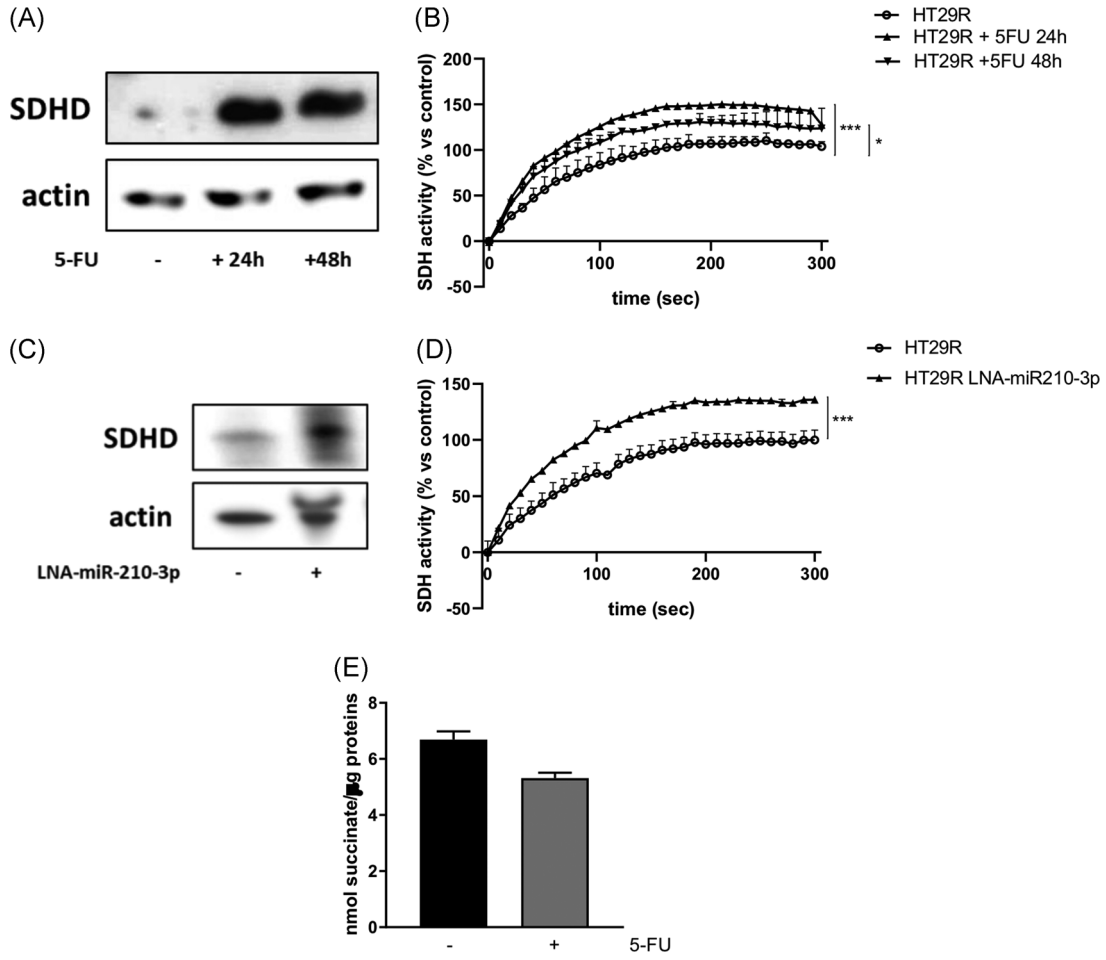

FIGURE 4 miR-210-3p regulates SDH increased activity in resistant cells after 5-FU treatment. (A) Representative western immunoblotting showing the levels of SDH subunits. HT29R cells were lysates after 24 or 48 hours of treatment with 20 μM 5-FU. An anti-actin antibody was used to ensure equal protein loading. (B) SDH activity measured on homogenates of HT29R cells previously treated with 20 μM 5-FU for 24 or 48 hours (data shown in mean ± SEM; two-way ANOVA, $^{*}P < .05$, $^{***}P < .001$; n = 3). (C) Representative western immunoblotting showing the levels of SDH subunits. HT29-resistant cells were transfected with LNA-miR-210 inhibitor. Twenty-four hours after the transfection, total proteins cells were subjected to Western blot analysis and detected for SDH subunits expression levels. An anti-actin antibody was used to ensure equal protein loading. (D) SDH activity measured on homogenates of HT29R cells after 24 hours of transfection with LNA-miR-210 inhibitor (data shown in mean ± SEM; two-way ANOVA, $^{***}P < .001$). (E) Quantification of intracellular level of succinate. Cells were treated with 5-FU for 24 hours. The amount of succinate inside the cells was quantified and plotted after protein normalization. (data were shown in mean ± SEM; unpaired *t* test, $^{**}P < .01$). SDH, succinate dehydrogenase

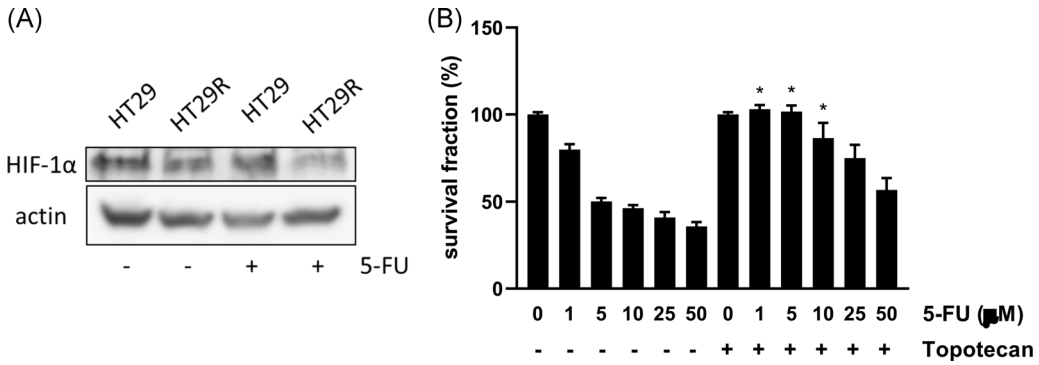

FIGURE 5 Decreased levels of HIF-1α mediate the resistant phenotype. (A) Representative western immunoblotting showing the levels of HIF-1α. HT29 and HT29R cells were lysates after 24 hours of treatment with 20 μM 5-FU. An anti-actin antibody was used to ensure equal protein loading. (B) HIF-1α inhibitor increases the resistance of HT29 sensible cells to 5-FU. HT29 cells were treated with an increasing amount of 5-FU for 72 hours, in presence or not of Topotecan (250 nM). After 72 hours of incubation, cells viability was evaluated using MTT assay (data were normalized respect to control test and shown in mean ± SEM; two-way ANOVA, $^{*}P < .05$). ANOVA, Analysis of Variance

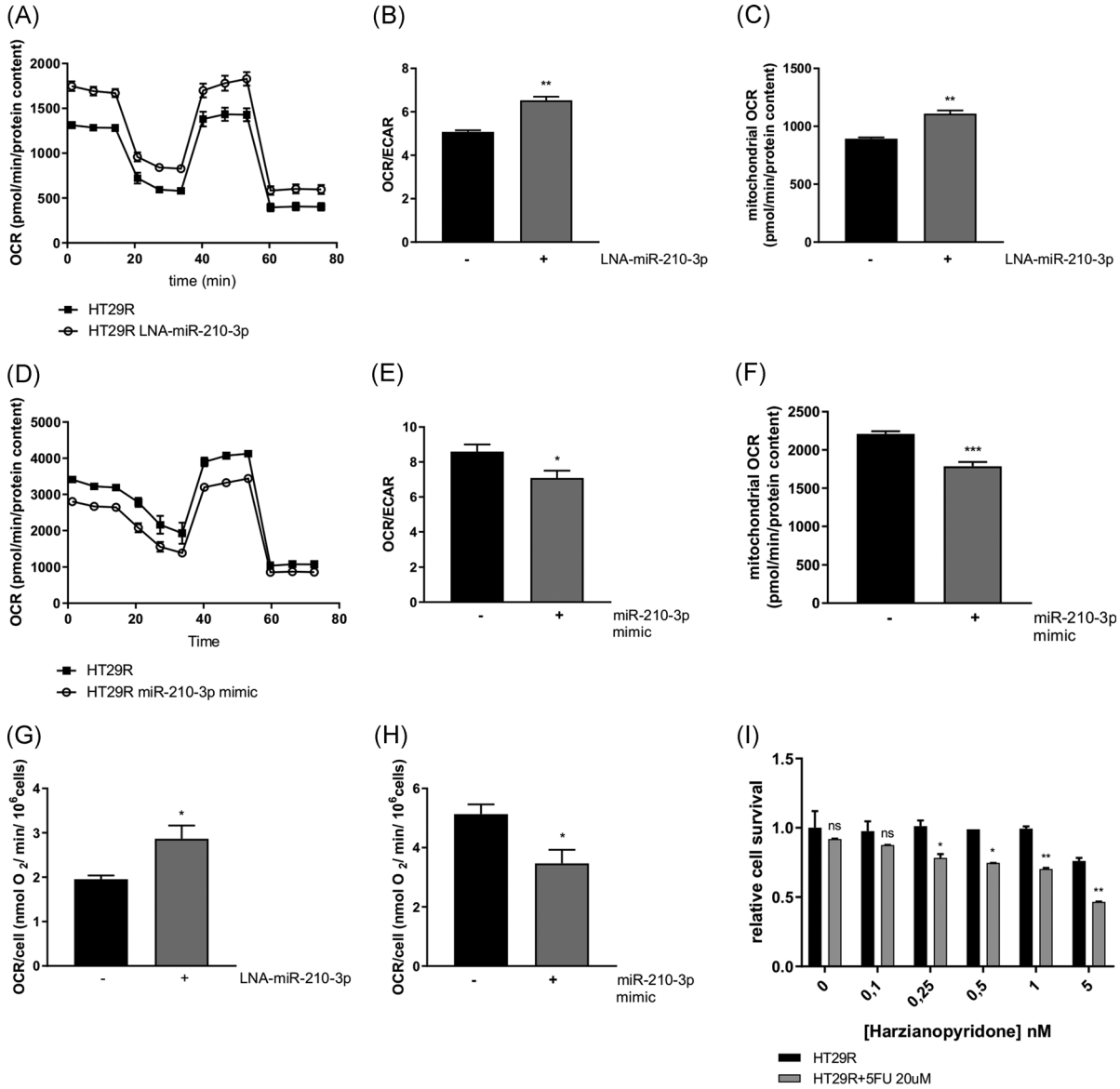

FIGURE 6 Metabolic adaptations mediated by miR-210-3p downregulation in resistant cells under acute treatment with 5-FU. Oxygen consumption rate (OCR) was evaluated by XF analysis performed under mitochondrial stress conditions in HT29R cells transfected with miR-210 LNA inhibitor 24 hours (A) or miR-210-3p mimic (D) before the analysis. (B, E) OCR/ECAR ratio in basal condition; (C, F) mitochondrial OCR obtained by subtraction of nonmitochondrial OCR from total basal OCR (data were shown in mean ± SEM; unpaired *t* test, $^{*}P < .05$, $^{**}P < .01$, $^{***}P < .001$). Oxygen consumption rate assessed with the Clark-type O_2 electrode in HT29R cells 24 hours after miR-210 LNA inhibitor (G) or miR-210-3p mimic transfection (H) (data were shown in mean ± SEM; unpaired *t* test, $^{*}P < .05$). (I) Cell viability assay of HT29R cells treated with increasing doses of the SDH inhibitor Harzianopyridone in combination with 20 μM 5-FU. After 48 hours or treatment, cell viability assayed with crystal violet staining (data were shown in mean ± SEM; two-way ANOVA, $^{*}P < .05$, $^{**}P < .01$). ANOVA, Analysis of Variance; ECAR, extracellular acidification rate; OCR, oxygen consumption rate; SDH, succinate dehydrogenase; XF, extracellular flux

specific cancer cell subpopulations, such as cancer stem cells, that are already present in the tumor mass before receiving chemotherapy. Conversely, cancer cells with acquired resistance can develop from sensitive cells during therapeutic treatment as consequence of genetic instability, mutations or various other adaptive responses.[29] Whatever the mechanism of development is present, resistant cancers cells are generally characterized by a strong plasticity that allows them to respond to many different stimuli, first of all, anticancer treatment.[30,31]

Even though in therapy drug administration generally lasts even after resistant cells are established in the tumor mass, little is known about the adaptations that resistant cells acquire during the treatment.

Understanding how resistant cells respond to the stress caused by drug exposure could help in the development of new approaches aimed at targeting specifically resistant cells during the treatment and progress to substantive improvements in patient outcomes.

In recent years, it has become evident that epigenetic control of gene expression, in particular through miRNA action, underpins both

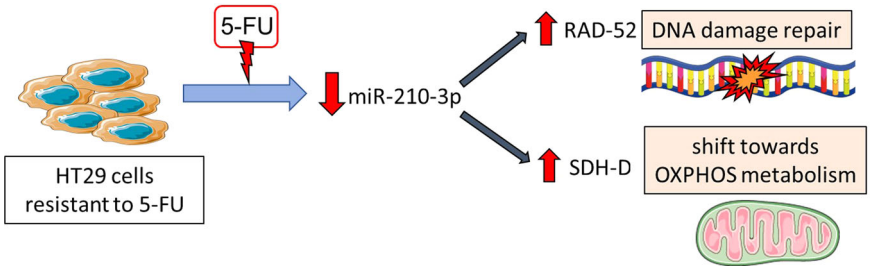

FIGURE 7 Diagrammatic summary of the molecular basis of miR-210-3p action in colon carcinoma cells. In colon cancer-resistant to 5-FU, the downregulation of miR-210-3p is instrumental to sustain DNA damage repair and metabolic adaptation following drug treatment [Color figure can be viewed at wileyonlinelibrary.com]

cancer development and drug resistance.[2,32] miRNAs are a class of small noncoding RNA molecules which negatively regulate the expression of selected targets by sequence-specific cleavage of mRNA or inhibition of translation.[33] Several miRNAs are located at the unstable genomic region, frequently subject to mutation.[34] For this reason, dysregulation of miRNA expression is frequently associated with cancer development and drug resistance acquisition.[35,36] A peculiar characteristic of miRNAs is the ability of only one miRNA to regulate simultaneously different target genes and multiple cellular processes. As a result, the alteration of one or a few miRNAs in response to a stimulus could consequently affect different pathways.[37] Targeting simultaneously different cellular adaptations in resistant cells could be a successful strategy to strike the plasticity that characterizes these cells.

For this reason, we investigated miRNAs modulation in a 5-FU-resistant HT29 cell line in response to drug exposure. Interestingly, in this resistance model, we found only four miRNAs differentially expressed following 5-FU exposure. The limited range of altered miRNAs following the treatment suggests that it could be possible to get a good sensitization of resistant cells to drug treatment by simply modulating few miRNAs levels.

In particular, we focused on miR-210-3p, a well-described miRNA implicated in different cellular processes such as hypoxia response, mitochondrial metabolism, angiogenesis as well as DNA repair and cell survival.[22] Notably, miR-210-3p is generally recognized as a target of hypoxia-inducible factor (HIF), and its overexpression has been associated with a genetic signature of hypoxia.[17] Despite its role in the cellular response to hypoxic conditions, miR-210-3p overexpression has been also described in a variety of solid tumors, even under circumstances of normoxia.[22] The miR-210-3p expression was found increased in numerous solid tumors, including breast cancer, non-small-cell lung cancer, head and neck cancer, pancreatic cancer, oral tumors, hepatocellular cancer, adrenocortical carcinoma, colon cancer, ovarian cancer, glioblastoma, malignant melanoma, renal cell cancer, and human esophageal squamous cell carcinoma tissues.[22,38,39]

Here we demonstrated a new role of miR-210-3p in the response to drug treatment of colon carcinoma cells already resistant to 5-FU. We found that 5-FU exposure induces a downregulation of miR-210-3p in resistant cells and that it is correlated with the ability of resistant cells to counteract drug action. Indeed, miR-210-3p downregulation allows an increase in DNA damage repair activity mediated by RAD-52, with consequent protection against drug action. Moreover, miR-210-3p downregulation also mediates an increase in SDHD expression, thus altering oxidative metabolism in resistant cells and inducing a shift towards OXPHOS. Our data demonstrated that all these adaptations, at least in part mediated by miR-210-3p, cooperate in the response implemented by resistant cells facing drug exposure (Figure 7).

These and several other works suggest that, besides identifying and directly targeting the proteins implicated in resistance pathways, it would be more effective to strive for deregulated miRNAs, to develop new miRNA-based therapies to overcome the survival of drug-resistance cells under continuous drug treatment.

ACKNOWLEDGMENTS

The work was supported by Associazione Italiana Ricerca sul Cancro (AIRC) (grant #8797). PP acknowledges AIRC for the project "Assaying tumor metabolic deregulation in live cells"; project code 19515.

CONFLICT OF INTEREST

The authors declare that there is no conflict of interest.

AUTHOR CONTRIBUTIONS

EP and AL designed and performed the experiments; ER, MR, FM, EG, and PC performed the experiments; MLT and PP contributed to the conception, design, and overall project management; AC, MLT, and PP wrote the manuscript.

ORCID

Maria Letizia Taddei http://orcid.org/0000-0002-6867-0620
Paolo Paoli http://orcid.org/0000-0001-6448-7266

REFERENCES

1. Holohan C, Van Schaeybroeck S, Longley DB, Johnston PG. Cancer drug resistance: an evolving paradigm. *Nat Rev Cancer*. 2013; 13(10):714-726.

2. Housman G, Byler S, Heerboth S, et al. Drug resistance in cancer: an overview. *Cancers (Basel)*. 2014;6(3):1769-1792.
3. Salgia R, Kulkarni P. The genetic/non-genetic duality of drug 'resistance' in cancer. *Trends Cancer*. 2018;4(2):110-118.
4. Melo SA, Esteller M. Dysregulation of microRNAs in cancer: playing with fire. *FEBS Lett*. 2011;585(13):2087-2099.
5. Zheng T, Wang J, Chen X, Liu L. Role of microRNA in anticancer drug resistance. *Int J Cancer*. 2010;126(1):2-10.
6. Ghasabi M, Mansoori B, Mohammadi A, et al. MicroRNAs in cancer drug resistance: basic evidence and clinical applications. *J Cell Physiol*. 2019;234(3):2152-2168.
7. Tournigand C, André T, Achille E, et al. FOLFIRI followed by FOLFOX6 or the reverse sequence in advanced colorectal cancer: a randomized GERCOR study. *J Clin Oncol*. 2004;22(2):229-237.
8. Denise C, Paoli P, Calvani M, et al. 5-Fluorouracil resistant colon cancer cells are addicted to OXPHOS to survive and enhance stem-like traits. *Oncotarget*. 2015;6(39):41706-41721.
9. Gee HE, Ivan C, Calin GA, Ivan M. HypoxamiRs and cancer: from biology to targeted therapy. *Antioxid Redox Signal*. 2014;21(8):1220-1238.
10. Taddei ML, Cavallini L, Comito G, et al. Senescent stroma promotes prostate cancer progression: the role of miR-210. *Mol Oncol*. 2014;8(8):1729-1746.
11. Franken NAP, Rodermond HM, Stap J, Haveman J, van Bree C. Clonogenic assay of cells in vitro. *Nat Protoc*. 2006;1(5):2315-2319.
12. Giovannelli L, Pitozzi V, Jacomelli M, et al. Protective effects of resveratrol against senescence-associated changes in cultured human fibroblasts. *J Gerontol A Biol Sci Med Sci*. 2011;66(1):9-18.
13. Rapizzi E, Fucci R, Giannoni E, et al. Role of microenvironment on neuroblastoma SK-N-AS SDHB-silenced cell metabolism and function. *Endocr Relat Cancer*. 2015;22(3):409-417.
14. Dang K, Myers K. The role of hypoxia-induced miR-210 in cancer progression. *Int J Mol Sci*. 2015;16(3):6353-6372.
15. De Angelis PM, Svendsrud DH, Kravik KL, Stokke T. Cellular response to 5-fluorouracil (5-FU) in 5-FU-resistant colon cancer cell lines during treatment and recovery. *Mol Cancer*. 2006;5:20.
16. Kuo LJ, Yang LX. Gamma-H2AX - a novel biomarker for DNA double-strand breaks. *In Vivo*. 2008;22(3):305-309.
17. Crosby ME, Kulshreshtha R, Ivan M, Glazer PM. MicroRNA regulation of DNA repair gene expression in hypoxic stress. *Cancer Res*. 2009;69(3):1221-1229.
18. New JH, Sugiyama T, Zaitseva E, Kowalczykowski SC. Rad52 protein stimulates DNA strand exchange by Rad51 and replication protein A. *Nature*. 1998;391(6665):407-410.
19. Chan SY, Zhang YY, Hemann C, Mahoney CE, Zweier JL, Loscalzo J. MicroRNA-210 controls mitochondrial metabolism during hypoxia by repressing the iron-sulfur cluster assembly proteins ISCU1/2. *Cell Metab*. 2009;10(4):273-284.
20. Puisségur MP, Mazure NM, Bertero T, et al. miR-210 is over-expressed in late stages of lung cancer and mediates mitochondrial alterations associated with modulation of HIF-1 activity. *Cell Death Differ*. 2011;18(3):465-478.
21. Selak MA, Armour SM, MacKenzie ED, et al. Succinate links TCA cycle dysfunction to oncogenesis by inhibiting HIF-α prolyl hydroxylase. *Cancer Cell*. 2005;7(1):77-85.
22. Devlin C, Greco S, Martelli F, Ivan M. miR-210: More than a silent player in hypoxia. *IUBMB Life*. 2011;63(2):94-100.
23. Wang H, Flach H, Onizawa M, Wei L, McManus MT, Weiss A. Negative regulation of Hif1a expression and TH17 differentiation by the hypoxia-regulated microRNA miR-210. *Nat Immunol*. 2014;15(4):393-401.
24. Mancini M, Gariboldi MB, Taiana E, et al. Co-targeting the IGF system and HIF-1 inhibits migration and invasion by (triple-negative) breast cancer cells. *Br J Cancer*. 2014;110(12):2865-2873.
25. Kummar S, Raffeld M, Juwara L, et al. Multihistology, target-driven pilot trial of oral topotecan as an inhibitor of hypoxia-inducible factor-1 in advanced solid tumors. *Clin Cancer Res*. 2011;17(15):5123-5131.
26. Beppu K, Nakamura K, Linehan WM, Rapisarda A, Thiele CJ. Topotecan blocks hypoxia-inducible factor-1α and vascular endothelial growth factor expression induced by insulin-like growth factor-I in neuroblastoma cells. *Cancer Res*. 2005;65(11):4775-4781.
27. Miyadera H, Shiomi K, Ui H, et al. Atpenins, potent and specific inhibitors of mitochondrial complex II (succinate-ubiquinone oxidoreductase). *Proc Natl Acad Sci*. 2003;100(2):473-477.
28. DeVita VT, Schein PS. The use of drugs in combination for the treatment of cancer: rationale and results. *N Engl J Med*. 1973;288(19):998-1006.
29. Longley D, Johnston P. Molecular mechanisms of drug resistance. *J Pathol*. 2005;205(2):275-292.
30. Doherty MR, Smigiel JM, Junk DJ, Jackson MW. Cancer stem cell plasticity drives therapeutic resistance. *Cancers (Basel)*. 2016;8(1):E8.
31. Poli V, Fagnocchi L, Zippo A. Tumorigenic cell reprogramming and cancer plasticity: interplay between signaling, microenvironment, and epigenetics. *Stem Cells Int*. 2018;2018:1-16.
32. Mansoori B, Mohammadi A, Shirjang S, Baradaran B. MicroRNAs in the diagnosis and treatment of cancer. *Immunol Invest*. 2017;46(8):880-897.
33. Bartel DP. MicroRNAs: target recognition and regulatory functions. *Cell*. 2009;136(2):215-233.
34. Calin GA, Sevignani C, Dumitru CD, et al. Human microRNA genes are frequently located at fragile sites and genomic regions involved in cancers. *Proc Natl Acad Sci*. 2004;101(9):2999-3004.
35. Lin S, Gregory RI. MicroRNA biogenesis pathways in cancer. *Nat Rev Cancer*. 2015;15(6):321-333.
36. Zhang Y, Wang J. MicroRNAs are important regulators of drug resistance in colorectal cancer. *Biol Chem*. 2017;398(8):929-938.
37. Kelly TK, De Carvalho DD, Jones PA. Epigenetic modifications as therapeutic targets. *Nat Biotechnol*. 2010;28(10):1069-1078.
38. McCormick R, Buffa FM, Ragoussis J, Harris AL. The role of hypoxia regulated microRNAs in cancer. *Curr Top Microbiol Immunol*. 2010;345:47-70.
39. Tsuchiya S, Fujiwara T, Sato F, et al. MicroRNA-210 regulates cancer cell proliferation through targeting fibroblast growth factor receptor-like 1 (FGFRL1). *J Biol Chem*. 2011;286(1):420-428.

SUPPORTING INFORMATION

Additional supporting information may be found online in the Supporting Information section.

How to cite this article: Pranzini E, Leo A, Rapizzi E, et al. miR-210-3p mediates metabolic adaptation and sustains DNA damage repair of resistant colon cancer cells to treatment with 5-fluorouracil. *Molecular Carcinogenesis*. 2019;1-12. https://doi.org/10.1002/mc.23107